

The Normal Force on a Planing Surface

Peter R. Payne*
Payne, Inc., Annapolis, Md.

The steady-state dynamic normal force acting on a planing plate is calculated from the downward velocity $u_0 \tau$ (the product of the freestream velocity and the trim angle) imparted to the virtual hydrodynamic mass associated with the plate's cross section. This virtual mass can, in principle, be evaluated for any plate cross section, although we currently have available values for only a limited range of shapes. When the chines are above the still water level, only the virtual mass term applies. When the chines are below the undisturbed water ("wet"), the Rayleigh-Kirchoff free-streamline crossflow force must be added to the virtual mass force. Despite the fact that there are no "constants determined from experiment," the agreement between theory and experiment, for the cases tested, is found to be excellent. The theory breaks down for very short wetted-length-to-beam ratios at low deadrise angles, because the virtual mass cannot be deflected through the full trim angle τ . For flat plates the lower end of this region is defined by two-dimensional theories to which a transition of the present theory is suggested. The basic theoretical approach was first presented in 1974, when it was shown that the theory permits the effect of pitch and heave transients to be computed, as well as steady-state forces for, in principle, any planing surface shape and camber, and, in principle, during maneuvers and in waves. The present paper constitutes a refinement of the analysis and, for the first time, a detailed comparison of its predictions with experimental data for steady-state planing.

Nomenclature

- A = aspect ratio = l/b for a flat plate
 b = total beam
 C_{DC} = crossflow force coefficient
 C_R = normal force coefficient = $R / \frac{1}{2} \rho u_0^2 S$
 $C_{R\tau}$ = $dC_R / d\tau$
 F = Froude number on wetted length = $u_0 \sqrt{gx_s}$
 g = acceleration due to gravity
 h = height of a rectangular prism, defined in Fig. 1
 l = distance between the transom heel and the point when the keel intersects the still water plane
 l_w = distance between the transom heel and the point at which the (piled up) water intersects the keel
 m'_x = maximum value of the virtual mass
 R = force normal to the planing surface
 S = plane of intersection with the water surface or the image on that plane of the *actual* water/hull intersection
 T = kinetic energy in the fluid
 u_0 = freestream velocity
 v = velocity normal to the freestream
 x = distance forward along the planing surface from the transom heel
 x_s = distance of stagnation line forward of the transom heel, measured along the keel in the case of a hull with deadrise
 y = semiwidth of the planing surface in water contact
 β = deadrise angle defined in Fig. 7
 ρ = mass density of the fluid
 τ = trim angle

Theory

THERE have been a number of attempts to calculate the normal force acting on a flat planing plate—some empirical fits to test data and some based on analogies with wings in an infinite fluid. Shuford¹ has provided a review of many of these, all of which are either totally empirical, or have empirical correction factors. More fundamental approaches have been reviewed by Pierson and Leshnover,¹⁹ and Mayo.³⁶

The concept of "virtual mass" is well established in hydro-nautics. It was first employed to predict the moments on bodies of revolution in an infinite fluid by Munk.² Jones³ later employed it to calculate the normal force on slender wings, in which he was followed by Ribner⁴ in his calculation of stability derivatives.

The first application to the planing problem was by von Kármán¹⁷ who suggested that the impact force on a seaplane hull during landing was a function only of the vertical v . For a prismatic bottom of dead-rise angle β and immersion z , he took the semiwidth of the hull as seen by the water to be instantaneously $y = z / \tan \beta$. Taking the virtual mass associated with this (per unit length) to be $\frac{1}{2} \rho \pi y^2$ (half the value for a lamina in an infinite fluid), he deduced that the vertical force F on the bottom should be

$$F = \frac{\rho v^2 \pi z}{\tan^2 \beta}$$

Early tests of von Kármán's equation were found to yield values that were too low. Pabst^{29,30} subsequently pointed out that this was because the velocity normal to the keel is not v but

$$v \cos \tau + u_0 \sin \tau$$

τ being the trim angle, and that, in general, the second term is much larger than the first. With this correction, the theory gave results of the same order as experiment.

Wagner^{16,31} who did not reference any previous workers, employed essentially the same methodology, but in more detail. Since he was using the virtual mass of a lamina, he assumed that the velocity of the free surface away from the bottom would be the same as that past a flat plate in an infinite fluid, and was thus able to compute its elevation. (While Wagner's surface elevation satisfies continuity,³⁷ the arc length of the surface does not satisfy the requirements of irrotationality.) This gave him a wetted width which was $\pi/2$ times the value of (y) previously used by von Kármán and Pabst, so that his force was greater by $\pi/2$ and his associated mass greater by $(\pi/2)^2$.

Wagner's work was later adapted by Pierson and Leshnover¹⁹ to the planing wedge problem, in a paper that has become a classic. In between Wagner and Pierson and Leshnover a number of workers (Mewes,³² Schmieden,³³

Submitted March 3, 1980; revision received March 6, 1981. Copyright © 1981 by P.R. Payne. Published by the American Institute of Aeronautics and Astronautics with permission.

*President. Member AIAA.

Sydow,³⁴ and Kreps³⁵) suggested relatively minor changes, mostly of an empirical nature, which could not be tested effectively against the meager and scattered data available at the time.

In 1974 Payne⁵ applied the concept to a heaving and pitching lamina, (following the lead of Ribner's⁴ analysis for slender wings) in order to study the "porpoising" (coupled pitch and heave) instability of planing hulls. More recent studies have been published by Zarnick⁴² and Martin.^{43,44}

The concept is very simple. If m' is the virtual mass per unit length associated with a semispan y ($m' = \rho \pi y^2$ for a flat plate in an infinite fluid) then the local normal force on the surface is given by†

$$\frac{dR}{dx} = \frac{d}{dt}(m'v) \quad (1)$$

where v is the transverse velocity imposed on the virtual mass. Since, in general,

$$\frac{dx}{dt} = -u_\theta \cos \tau \approx -u_\theta \quad (2)$$

τ being the local angle of the surface to the freestream velocity vector u_θ , we may transform Eq. (1) to

$$\frac{dR}{dx} = v \frac{dm'}{dt} + m' \frac{dv}{dt} = -vu_\theta \frac{dm'}{dx} + m' \frac{dv}{dt} \quad (3)$$

The second term in Eq. (3) gives force proportional to heave and pitch acceleration.⁵ The first term gives the heave and pitch velocity dependent terms and a "steady state" term

$$\frac{dR}{dx} = -\tau u_\theta^2 \frac{dm'}{dx} \quad (4)$$

For the case of zero camber, we can integrate Eq. (4) immediately to get, for the total normal force,

$$R = -\tau u_\theta^2 \int_0^{x_s} \frac{dm'}{dx} dx = \tau u_\theta^2 m'_x \quad (5)$$

where m'_x is the maximum value, occurring (usually) at the maximum span. (For a discussion of this see p. 98 of Ref. 15. Equation (5) merely states that $R = \dot{m} \Delta v$ where \dot{m} is the mass flow and Δv the vertical velocity change imposed on it.)

If the surface is cambered the integral of Eq. (3) can be written as

$$\begin{aligned} R &= -u_\theta^2 \int_0^{x_s} \left[\tau \frac{dm'}{dx} + m' \frac{d\tau}{dx} \right] \cos(\tau - \tau_x) dx \\ &\approx -u_\theta^2 \int_0^{x_s} \left[\tau \frac{dm'}{dx} + m' \frac{d\tau}{dx} \right] dx \text{ for small } (\tau_s - \tau_x) \end{aligned}$$

Integrating by parts, we obtain

$$R = u_\theta^2 \tau_x m'_x$$

That is, the force is defined by the virtual mass at the transom and the angle τ_x through which it is deflected, a result which we might have anticipated. As shown by Payne,⁵ the

†In the usual notation, the kinetic energy of the fluid due to a body's rectilinear motion is $T = \frac{1}{2} m' v^2$. Thus, if a force R acts on the body in the direction of motion,

$$Rv = \frac{dT}{dt} = m'v \frac{dv}{dt} \text{ or } R = m' \frac{dv}{dt}$$

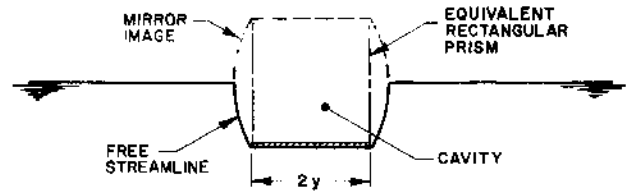


Fig. 1 Cross-sectional representation of parallel-sided planing plate.

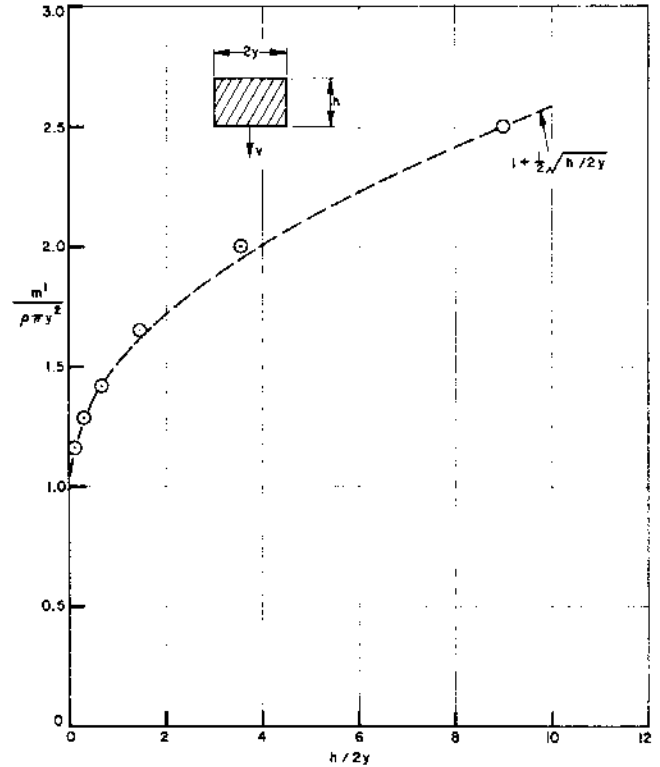


Fig. 2 Virtual mass of a rectangular prism in an infinite fluid (from Taylor⁸). The "data points" are from exact numerical computations of Taylor. The curve is an empirical fit to them.

principal effect of camber is to reduce the induced drag, the maximum reduction possible being 50%.

A parallel-sided planing plate can be approximately represented, in section, as in Fig. 1. To compute the normal force, we therefore need to know the virtual mass associated with the plate and the cavity that it produces in the water. Unfortunately, this is not yet known, although it will clearly be of the order of $\frac{1}{2} \rho \pi y^2$. The best approximation in the literature is for a rectangular prism, quoted by Kennard⁶ and due to Riabouchinsky⁷ and Taylor.⁸ As shown in Fig. 2, an acceptable analytic function for this is

$$m' / \rho \pi y^2 = 1 + \frac{1}{2} \sqrt{h/2y} \quad (6)$$

in an infinite fluid. For a planing plate we take half this value.

For a parallel plate with a stagnation line at a distance x_s from the trailing edge, the local value of h (including the mirror image) is

$$2(x_s - x)\tau$$

Thus,

$$m' = \frac{1}{2} \rho \pi y^2 \left[1 + \frac{1}{2} \sqrt{\frac{\tau}{y} (x_s - x)} \right] \quad (7)$$

Substituting into Eq. (5) the virtual mass reaction force is

$$\Delta R = \frac{1}{2} \rho u_\theta^2 \tau \pi y^2 \left[1 + \frac{1}{2} \sqrt{\tau x_s / y} \right] \quad (8)$$

The term $\frac{1}{2}\rho u_0^2 \pi y^2$ is the so called "linear term" in slender wing theory (reduced by one half for the planing problem) and referred to by Payne⁵ as the "stagnation line lift" term, while

$$\frac{1}{2}\rho u_0^2 (\pi/2) \tau^{3/2} \sqrt{x_s y^3}$$

is a nonlinear term that has no counterpart in slender wing theory. Its occurrence in the theory explains why attempts to curve fit functions like $C_R = A\tau + B\tau^2$ or $C_R = A\tau^n$ have been unsuccessful.

There is also a "cross-flow term" not identified by the von Kármán/Jones analysis. In an infinite fluid we can see from Eq. (4) that, if y is locally constant ($dy/dx=0$) so that $dm'/dx=0$, then $dR/dx=0$ no matter what the trim angle τ . In fact, due to vortex shedding, there will be a local normal force proportional to

$$\frac{1}{2}\rho u_0^2 \cdot 2y \cdot \sin^2 \tau \quad (9)$$

In the planing problem there is no shed vorticity (the flow is irrotational) and there is no known solution for the cross-flow field. But when the plate is deep in the water it is reasonable to assume that the crossflow can be approximated by the Rayleigh-Kirchoff free streamline flow around a flat plate[†] for which the plate force coefficient is

$$C_{DC} = 2\pi / (4 + \pi) \approx 0.88 \quad (10)$$

For shallow immersions, the use of this value represents an assumption only justifiable by the achievement of good agreement with experiment. [In so far as we can truncate the Rayleigh-Kirchoff flow and place an image above the surface (there will be discontinuities in the first derivative) we note with Taylor⁸ that the special boundary conditions appropriate to a free surface are automatically fulfilled at an axis of symmetry, for motion normal to the surface. This is also implied in Wagner's¹⁶ analysis, of course.]

As noted by Shuford and other investigators, the value of C_{DC} is reduced if the plate chines are not absolutely sharp, due to partial flow attachment around them (Coanda effect). It is also possible to have plate planforms where the flow does not separate from the chines at all, an example being a triangular wedge, vertex forward^{21,22} and in this case we would expect $C_{DC} \approx 0$ from the well-known proof that the axial force on a semi-infinite body is zero.

Figure 3 shows an effect not previously noted—namely, that the virtual mass deflection force is also reduced by rounded chines. An analogous reduction would be expected if the flow separates at the chines and then reattaches above them, because the separation bubble would then become part of the shape generating the virtual mass integral.

Thus, finally the dynamic normal force coefficient on wetted area (S) for a parallel-sided flat plate, following the preceding reasoning, would be (for sharp chines)

$$C_R = \frac{R}{\frac{1}{2}\rho u_0^2 S} \approx \frac{\pi y}{2x_s} \left[1 + \frac{1}{2}\sqrt{\tau x_s/y} \right] + C_{DC}\tau^2 \quad (11)$$

Clearly, as $x_s \rightarrow 0$, $C_R \rightarrow \infty$ in this formulation. The model breaks down as the limit is approached because, for short wetted lengths x_s , the full virtual mass m' cannot in fact be deflected through the angle (τ). Or put another way, the virtual mass is less than the two-dimensional value for very short wetted lengths.

[†]Lamb,⁹ Art. 76 gives this solution for a flat plate. Korvin-Kroukovsky and Chabrow¹⁸ have presented solutions for the (deeply submerged) free streamline flow past surfaces with deadrise. For deadrise angles $\beta = 10, 20$, and 30 deg they give $C_{DC} = 0.818, 0.796$, and 0.732 , respectively.

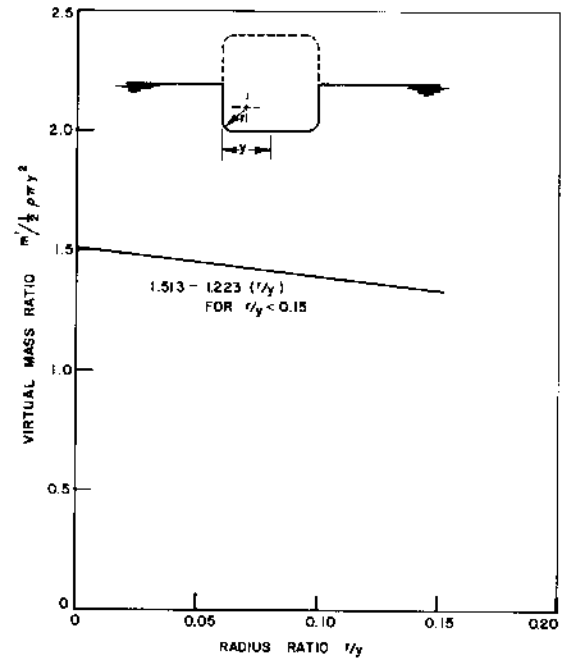


Fig. 3 Virtual mass for a square prism with radiused corners (after Taylor⁸).

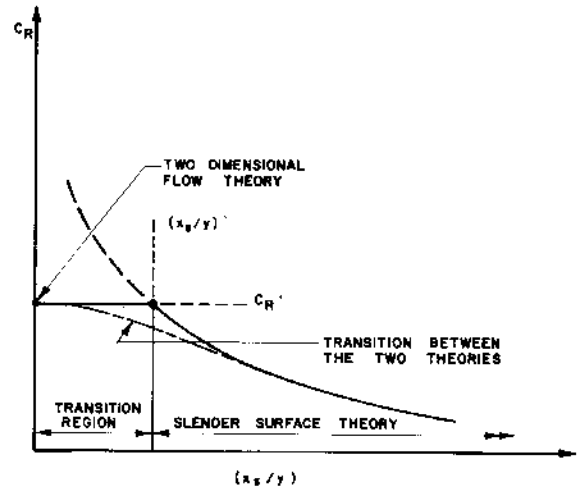


Fig. 4 The two different planing regimes.

There is, in fact, a limiting value to the value of C_R which we know to be for very small trim angles $C_R \approx \pi\tau$ from the work of Sedov¹⁰ and Squire¹¹ in their analyses of a two-dimensional planing plate. More precisely, the small angle limiting value is $C_R = \pi\tau f(F)$ where the function $f(F)$ of Froude number $F = u_0/\sqrt{gx_s}$ is always less than unity except in the limit $F \rightarrow \infty$.

For trim angles in excess of a few degrees C_R is somewhat less than $\pi\tau f(F)$. The only large angle solutions known to the writer, those of Sedov¹⁰ and Pierson and Leshnover²⁷ are for infinite Froude number, although Payne^{12,28} has suggested an empirical Froude number correction based on small angle theory, resulting in

$$C_R = \frac{2\pi}{\left[\pi + \cot \frac{\tau}{2} + \tan \frac{\tau}{2} \log \left(\cot^2 \frac{\tau}{2} - 1 \right) \right] \left[1 + \frac{5}{8} \frac{\pi}{F^2} \right]} \quad (12)$$

We shall see later that there is little point in employing the Froude number correction since Eq. (12) only applies in the limit of $\ell_w/b \rightarrow 0$ and hence $F \rightarrow \infty$.

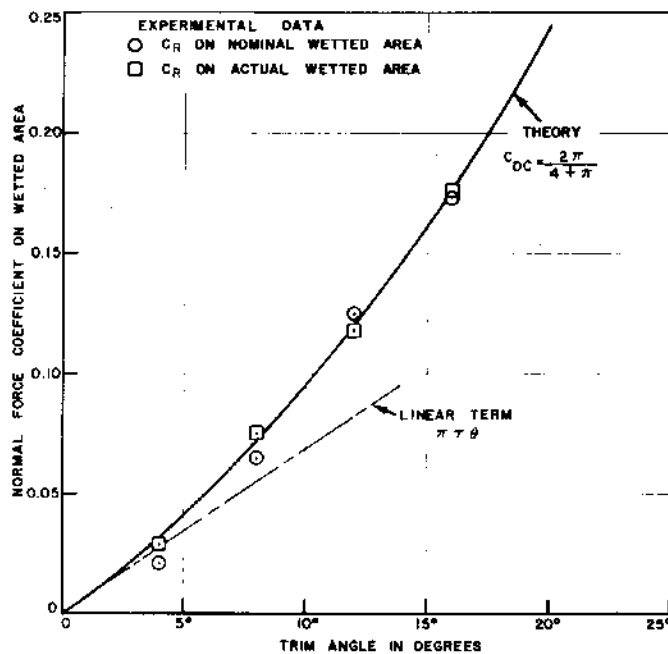


Fig. 5 Comparison between theory and the experiments of Wadlin and McGehee¹³ ($\tan \theta = 0.125$).

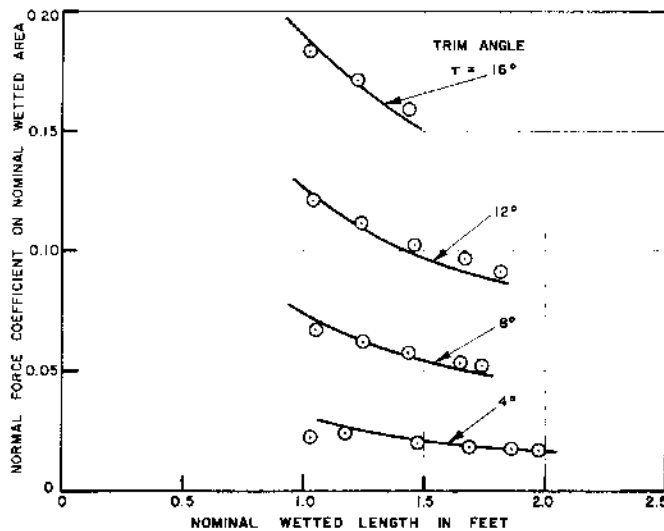


Fig. 6 Comparison between theory ($C_{DC} = 0.88$) and experiment for the flat plate ski tested by Wadlin and McGehee.¹³ (Nominal wetted length is given by the intersection with the still-water surface.)

We therefore have two models for the planing process. The first is for high length-to-beam ratios, and the second is for very low length-to-beam ratios. As a first order of approximation we might assume that the junction of these two regions occurs where they both predict the same value of C_R , as indicated in Fig. 4.

Thus we now have a model in which, when

$$0 < (x_s/y) < (x_s/y)^*$$

C_R is roughly constant with x_s/y and when

$$(x_s/y) > (x_s/y)^*$$

C_R falls with increasing x_s/y in accordance with Eq. (11).

In practice, of course, there must be a smooth transition between the two theories. Although the concept of "aspect ratio" makes no sense in the context of bound vortices (the

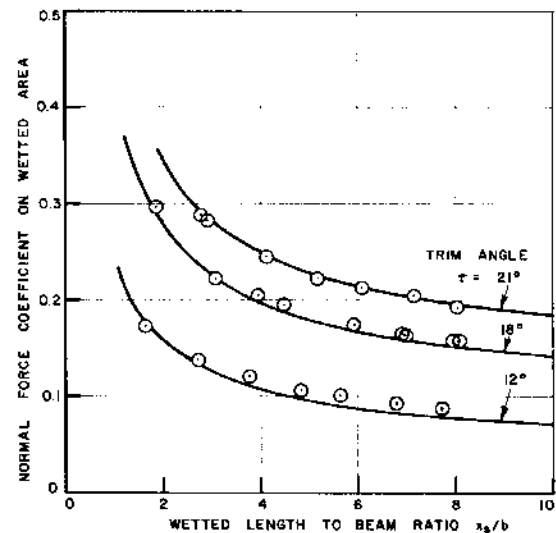


Fig. 7 Comparison of Eq. (11) ($C_{DC} = 0.88$) with the sharp-chine flat-plate data of Shuford.¹ (Based on actual wetted length because Shuford does not report draft. The difference is not large at high length-to-beam ratios.)

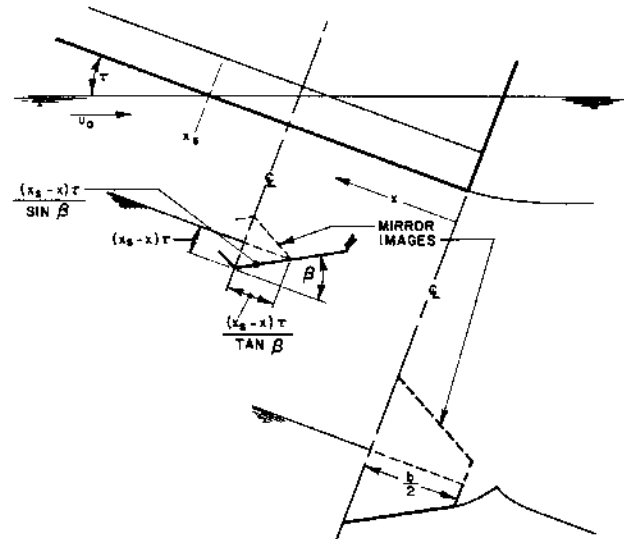


Fig. 8 A planing surface with deadrise.

flow is irrotational), it is clear that the sideways loss of water from the spray root will reduce the lift from the two-dimensional value, as indicated by the transition curve in Fig. 4.

If only the stagnation line force in Eq. (11) were considered, and the value of $C_{R\tau} = \pi$ were used for two-dimensional flow, then the critical value of x_s/y at which the theories intersected would be

$$(x_s/y)^* = 1/2 \quad (13)$$

implying the surprisingly large aspect ratio of 4. In practice, the critical value of (x_s/y) separating the two regions is obtained by equating Eqs. (11) and (12). And on either side of this critical value, either Eq. (11) or (12), as appropriate, gives the normal coefficient.

So far several tests have been applied to the theory for flat plates. The simplest was a triangular ski (vertex aft) tested by Wadlin and McGehee.¹³ In this case only the stagnation line lift can exist (no term in $\tau^{3/2}$) because the maximum virtual mass occurs at the stagnation line. As Fig. 5 (taken from Ref. 14) shows, the agreement between theory and experiment is generally excellent. The coefficient based on nominal wetted length (still water intersection) is low for $\tau = 4$ deg because,

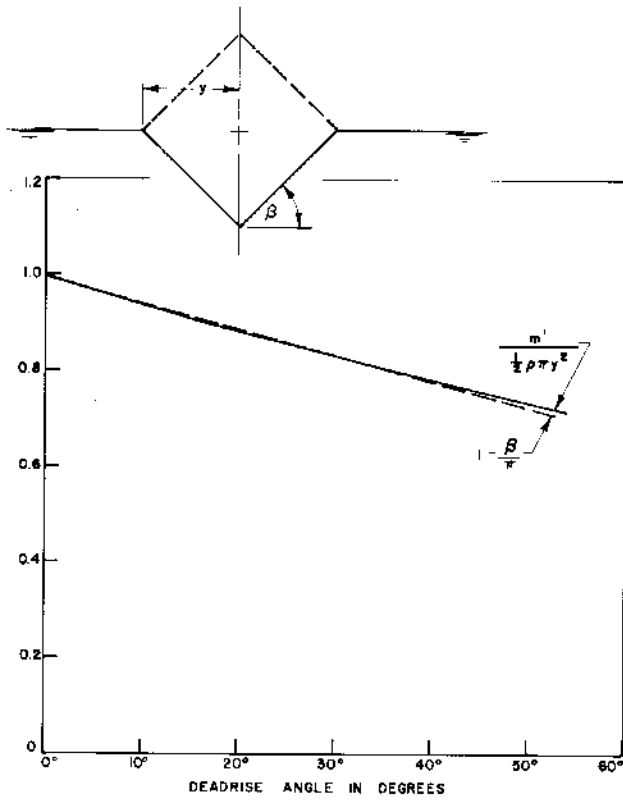


Fig. 9 Virtual mass coefficient for a rhombic cylinder (after Taylor⁸).

with this type of surface, the water is depressed in front of it at low trim angles, according to Wadlin and McGehee.

Figure 6 shows a comparison for parallel-sided ski with a triangular platform taper over its rear half. The data in Fig. 6 are limited to cases when the triangular aft end is totally immersed. The agreement between theory and experiment is again considered to be excellent. Figure 7 shows a comparison with the high trim angle flat plate data of Shuford.¹

When the planing surface has deadrise, the situation will be as shown in Fig. 8. For the *chines dry* case the width of the nominal water intersection at the transom will be

$$x_s \tau / \tan \beta \quad (14)$$

and, hence, from Eq. (5) the normal force will be

$$R = \tau u_0^2 m'_x$$

where

$$m'_x = (\frac{1}{2} \rho \pi y^2) f(\beta)$$

and

$$f(\beta) = \frac{1}{\pi \cos^2 \beta} \left[\frac{\pi(\pi - 2\beta)}{[\Gamma(\frac{1}{2} + \beta/\pi) \Gamma(1 - \beta/\pi)]^2} - \sin 2\beta \right]$$

from Taylor⁸ §

$$\therefore R = \frac{1}{2} \rho u_0^2 \pi \left(\frac{x_s \tau}{\tan \beta} \right)^2 \tau f(\beta) \quad (15)$$

§Ferdinand²⁶ who was apparently unaware of the work of Taylor,⁸ presents values for m' which are over twice the flat plate values for low values of β and are lower than Taylor's values at high deadrise angles. He makes no comparisons with experiment. Bisplinghoff,⁴⁰ who was also unaware of Taylor's work, obtains the correct result using three different analytical procedures. He also cites Monaghan⁴¹ as having obtained essentially the same result. Kreps³⁵ quotes a similar solution by Sedov and notes that $f(\beta) = 1 - \beta/\pi$ very closely for small angles. In fact, it is quite good for all angles.

Table 1 Values of $f(\beta)$

β , deg	$f(\beta) = m' / \frac{1}{2} \rho \pi y^2$
9	0.94221
18	0.89031
36	0.80121
45	0.75660
54	0.71639

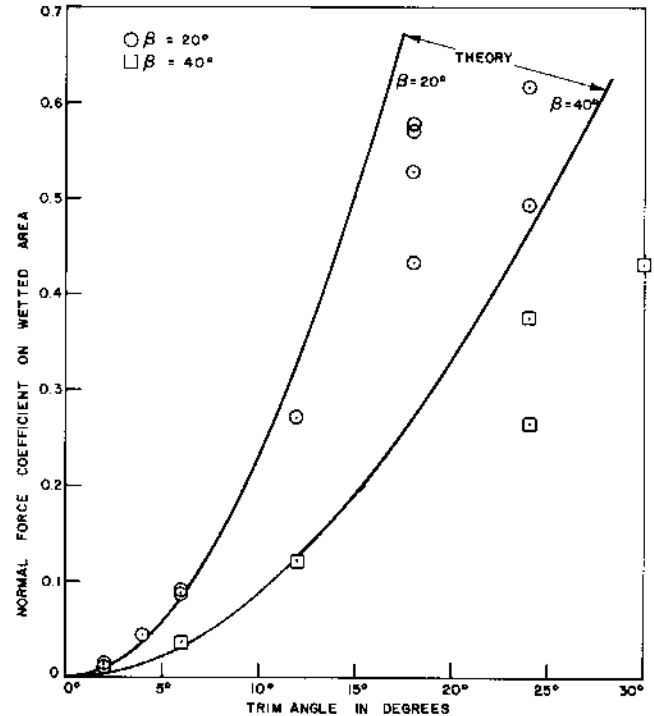


Fig. 10 Equation (17) compared with the dry-chine data plane of Chambliss and Boyd.²³ (The theory is based on nominal water plane intersection area; the data on actual (photographed) wetted area, which is greater at large trim angles.

Values of $f(\beta)$ are plotted in Fig. 9 and listed in Table 1. Dividing Eq. (15) by $\frac{1}{2} \rho u_0^2 b^2$ leads to

$$C_{Rb} = \frac{R}{q_0 b^2} = \frac{\pi \tau^3}{\tan^2 \beta} \left(\frac{x_s}{b} \right)^2 f(\beta) \quad (16)$$

and

$$C_R = \frac{\pi f(\beta) \tau^2}{\tan \beta} \quad (17)$$

since

$$S = x_s^2 \tau / \tan \beta$$

It is interesting to note that, from Eq. (17), C_R on the wetted area (actually the plane of intersection with the water surface) is independent of wetted area. Since the shape is self-similar, no matter what the scale (value of x_s/b) it would be very surprising if this were not so, but the writer has not noticed any use of this in the analysis of test data.

A second surprise is that $C_R \propto \tau^2$, rather than linearly with τ , because the change of stagnation line sweep with τ results in an increase in aspect ratio with an increase in τ , and an increase in stagnation line lift. Since most investigators¹ assume a linear dependence a priori their difficulties in obtaining good correlation are now understandable.

A test of Eq. (17) can be made, but unfortunately not a very precise one. The fairly recent data of Chambliss and Boyd²³ is presumably accurate, but no measurements of draft were re-

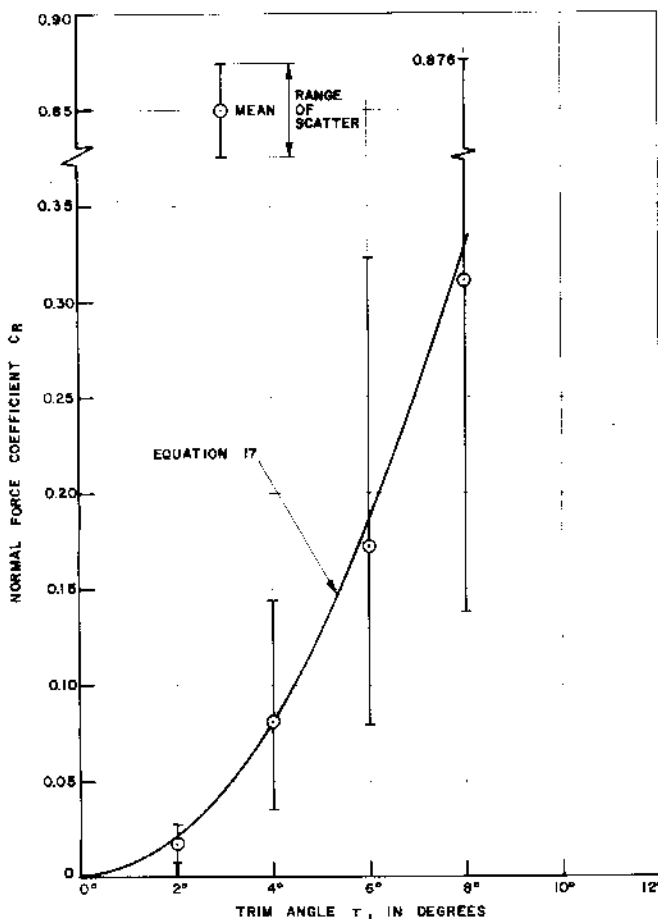


Fig. 11 Shoemaker's³⁹ dry-chine data for a deadrise angle of $\beta = 10$ deg.

corded in the data listing, so that the water-plane intersection cannot be computed. Plotting C_R based on actual wetted area (Fig. 10), therefore, gives data points which agree with the theoretical lines at low trims, but are substantially under them at high trims.

Shoemaker's³⁹ data for deadrise angles $\beta = 10, 20$, and 30 deg (Figs. 11-13) do not suffer from this defect, but his experimental equipment seems to have been very crude (not surprisingly, in 1934) so that the data are very scattered. But, as Figs. 11-13 show, the theoretical lines do more or less pass through the mean of his data points, and at least clearly validate that $C_R \propto \tau^2$.

Sottorf's^{20,38} flat-plate data is also useful in showing the Fig. 4 transition from two-dimensional flow to slender planing surface flow. In Fig. 14 we have divided his lift data (also divided by $\cos \tau$) into Eq. (11). For aspect ratios greater than unity we are clearly in the "slender surface" region.

In Fig. 15, we have divided Sottorf's data into Eq. (12) without the Froude correction. The result indicates that two-dimensional theory is strictly valid (as we would expect) only in the limit of $l/b \rightarrow 0$. The "fairing" curve between this limit and slender surface theory is given by the empirical fit

$$C_R = \frac{C_{R2-D}}{1 + kl/b} \quad (18)$$

where $k \approx 3.7$.

Pressure Distributions

A defect of a virtual mass theory of planing is that it does not enable a detailed pressure distribution to be calculated; but it does not preclude an approximation, which is often

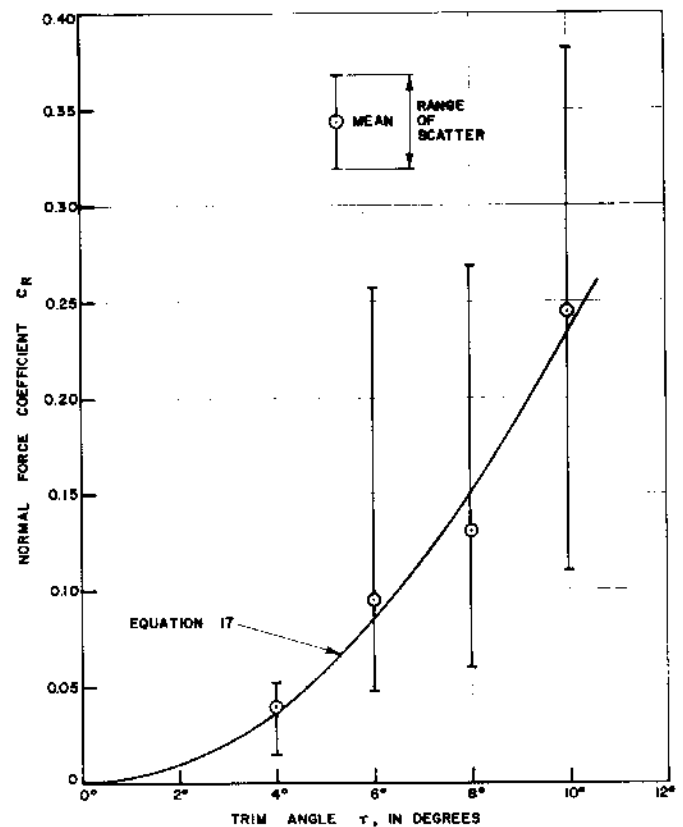


Fig. 12 Shoemaker's³⁹ dry-chine data for a deadrise angle of $\beta = 20$ deg.

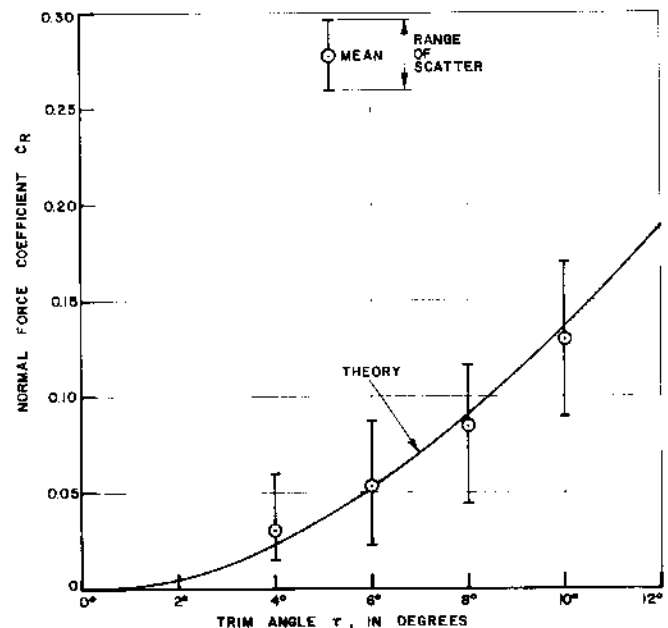


Fig. 13 Shoemaker's³⁹ dry-chine data for a deadrise angle of $\beta = 30$ deg.

adequate for engineering purposes. A typical approximation for a flat plate (the simplest of several alternatives) is shown in Fig. 16.

The equations presented for a flat plate, for example, give a "stagnation line force," a distributed virtual mass force, and a distributed crossflow force. Since the pressure coefficient

$$C_p = \Delta p / \frac{1}{2} \rho u_0^2$$

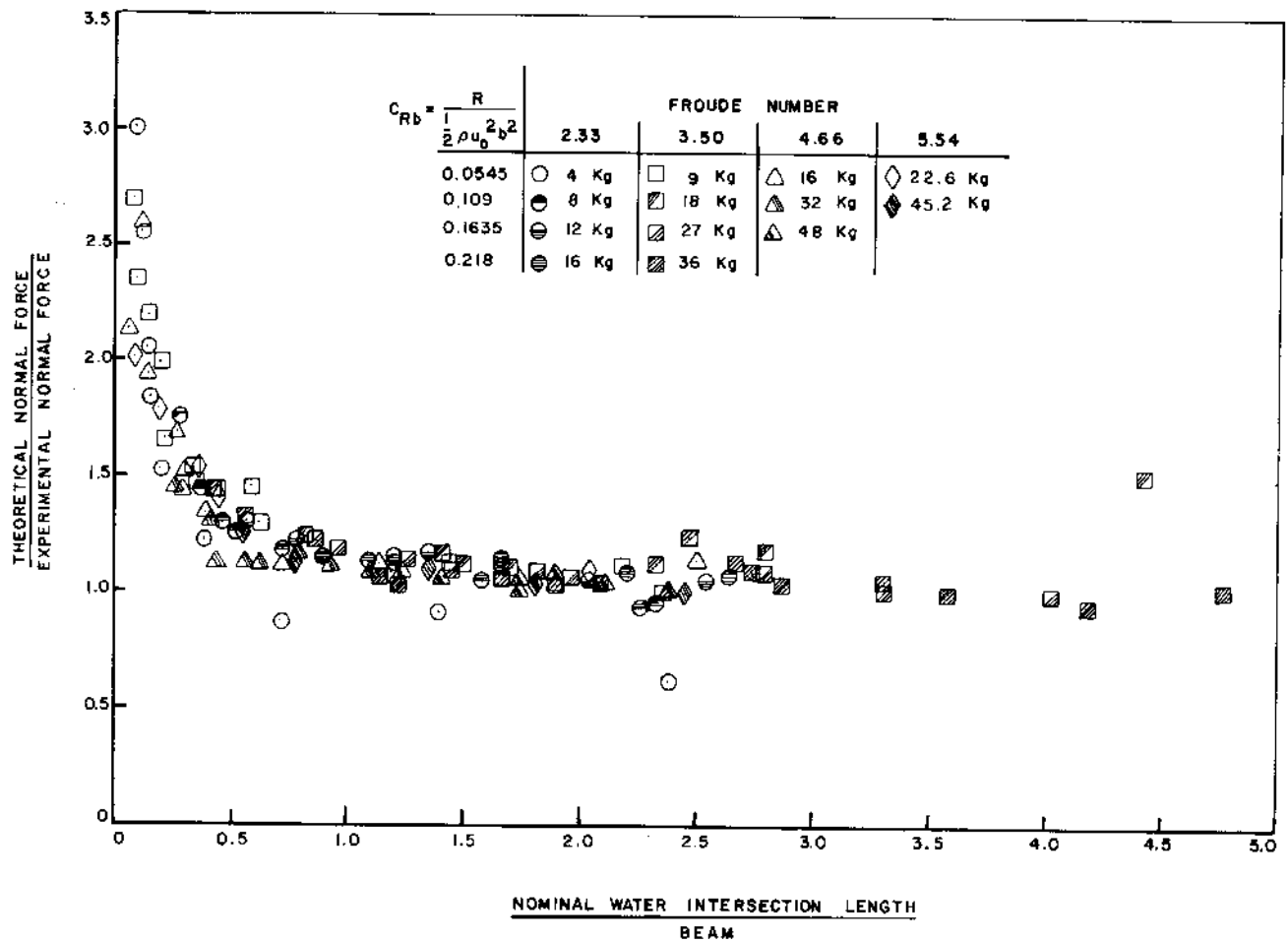


Fig. 14 Sottorf's³⁸ flat-plate data divided into Eq. (11) for a flat slender planing surface.

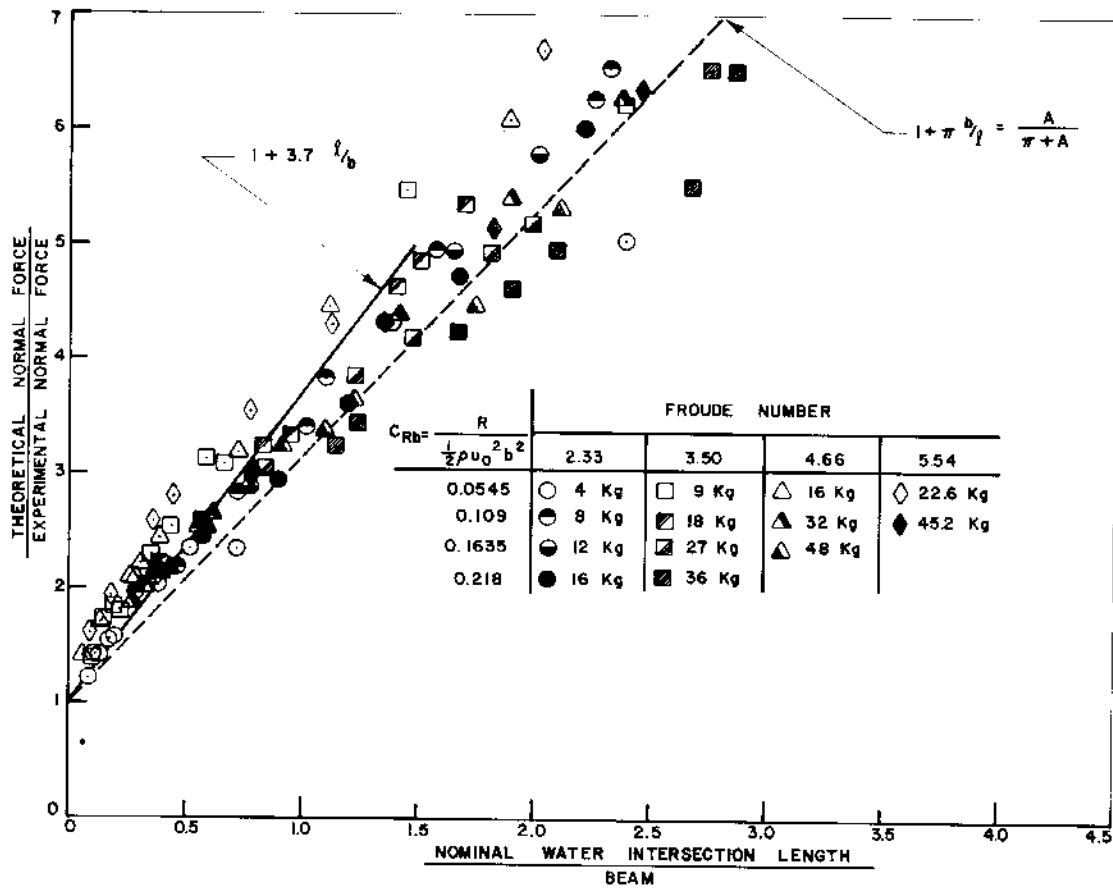


Fig. 15 Equation (12) divided by Sottorf's³⁸ flat-plate normal force data.

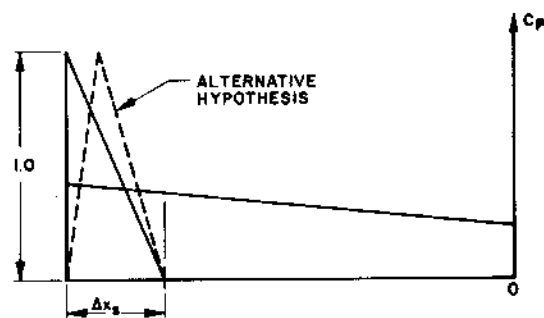
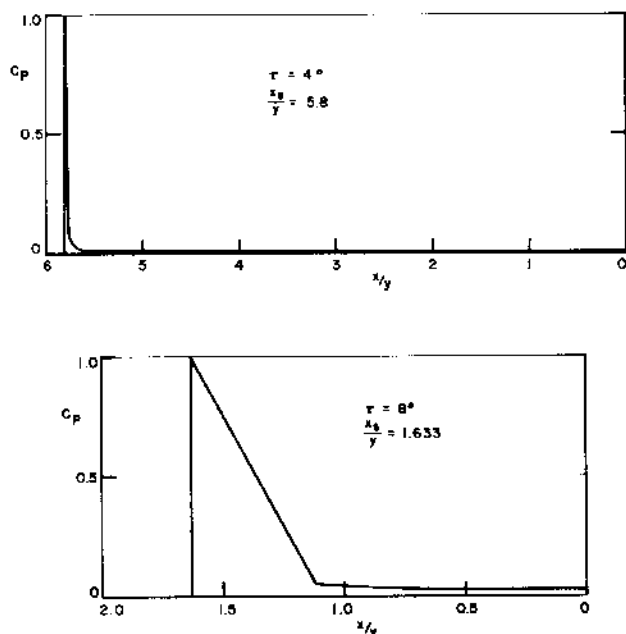


Fig. 16 Idealized pressure distribution.

Fig. 17 Theoretical flat-plate pressure coefficient distributions for two cases tested by Sottorf.³⁸

cannot exceed unity (at the stagnation line) we can approximate the forward portion of the pressure distribution as a triangle, i.e.,

$$\begin{aligned}\Delta R_F &= \frac{1}{2} \rho u_0^2 y \Delta x_s \\ &= \frac{1}{2} \rho u_0^2 \pi \tau y^2 \left[1 + \frac{1}{2} \sqrt{\tau \Delta x_s / y} \right] + \frac{1}{2} \rho u_0^2 2y \Delta x_s C_{DC} \tau^2\end{aligned}$$

which leads to

$$(1 - 2C_{DC}\tau^2) \frac{\Delta x_s}{y} - \frac{\pi}{2} \tau^{3/2} \sqrt{\frac{\Delta x_s}{y}} - \pi \tau = 0 \quad (19)$$

which can be solved for $\Delta x_s/y$. The rear portion of the pressure distribution is given by

$$\begin{aligned}C_P &= \frac{l}{2y} \frac{1}{\frac{1}{2} \rho u_0^2} \frac{dR}{dx} = \frac{\pi}{8} \frac{\tau^{3/2}}{\sqrt{(x_s - x)/y}} + C_{DC} \tau^2 \\ &\quad x > (x_s - \Delta x_s) \quad (20)\end{aligned}$$

Pressure distributions for two cases measured by Sottorf³⁸ are given in Fig. 17 using this methodology. They are not unlike Sottorf's experimental distributions when his hydrostatic pressure is subtracted. However, Sottorf's pressure data should be treated with caution since his peak (stagnation) pressures are between 24 and 32% of the actual stagnation pressure associated with the towing speed.

For a prismatic hull the stagnation line is swept back at an angle to the flow of ξ given by (from Fig. 8)

$$\tan \xi = \tau / \tan \beta$$

The velocity component normal to the stagnation line is, therefore, $u_0 \sin \xi$ so that the maximum pressure coefficient is approximately

$$C_{PM} = \sin^2 \xi = \tau^2 / (\tau^2 + \tan^2 \beta) \quad (21)$$

Comparing Eqs. (21) and (17) we see that the "form factor"

$$\Phi = C_R / C_{PM}$$

of the lateral pressure distribution may be greater or less than unity, being less than one for combinations of small trim angles and small deadrise angles. This generally agrees with the meager static pressure data available in the literature (see, for example, Kapryan and Boyd²⁵).

Conclusions

1) To at least the same accuracy as empirical curve fits, the steady-state normal force on a planing surface can be calculated from known hydrodynamic principles. It follows that transient forces and moments due to heave and pitch rate and acceleration can also be computed, as well as the effects of geometric variations such as camber⁵ and the change of forces during maneuvers.⁵ (The relationship between virtual mass and forces during transient motions in three degrees of freedom has been given by Sedov.²⁴)

2) For the chines-immersed case there is some loss of precision due to not knowing the exact virtual mass expression for the cavity shape. Neither do we know the values for any shape in nonsymmetric (maneuvering) motion. This should be rectifiable, since there exist both numerical schemes and electric and mechanical analogues for determining the virtual mass of arbitrary shapes. Alternatively, having established the validity of the theory, we can work backward from experimental data.

3) Although the normal force on a two-dimensional flat planing plate is Froude-number dependent, this does not appear to be the case for high length-to-beam ratios.

4) Although there is a widespread belief that a knowledge of the water surface elevation in the stagnation region is important to the calculation of dynamic lift (see, for example, the notable studies of Pierson and Leshnover¹⁹) and that test data should be nondimensionalized by actual (photographed) wetted area rather than the nominal still-water intersection plane, this is still an open question so far as the present study is concerned.

Present indications are that this is only true for high-aspect-ratio flat plates, where the available theory (Pierson and Leshnover²⁷) is derived in terms of wetted length rather than nominal intersection length, because the latter cannot be deduced from the theory.

5) Crude approximations to the pressure distribution can be derived, even though virtual mass theories notoriously provide little information on this aspect of the problem.

6) The normal force coefficient of a flat plate varies with trim angle τ as $A\tau + B\tau^{3/2} + C\tau^2$. The linear term is due to the lift developed at the stagnation line, which (for a flat plate) is always normal to the flow. For a surface with deadrise, in the chines-dry case, C_R varies as $A\tau^2$. There is no linear term like that of the flat plate because the sweep of the stagnation line changes with changing trim. That is to say, with increasing trim the stagnation line becomes less swept (which increases its lift) and the aspect ratio of the wetted plane increases. Presumably a term like $\tau^{3/2}$ would be added when the chines are immersed, but this cannot be resolved until the virtual mass for the appropriate cavity cross section has been determined; perhaps using the work of Korvin-Kroukovsky and Chabrow¹⁸ as a starting point.

References

- ¹Shuford, C.L., "A Theoretical and Experimental Study of Planing Surfaces Including Effects of Cross Section and Plan Form," NACA 1335, 1958.
- ²Munk, M.M., "The Aerodynamic Forces on Airship Hulls," NACA 184, 1924.
- ³Jones, R.T., "The Properties of Low-Aspect Ratio Pointed Wings at Speeds Below and Above the Speed of Sound," NACA TN 1032, 1946.
- ⁴Ribner, H.S., "The Stability Derivatives of Low-Aspect Ratio Triangular Wings at Subsonic and Supersonic Speeds," NACA TN 1423, 1947.
- ⁵Payne, P.R., "Coupled Pitch and Heave Porpoising Instability in Hydrodynamic Planing," *Journal of Hydronautics*, Vol. 8, April 1974, pp. 58-71.
- ⁶Kennard, E.H., "Irrotational Flow of Frictionless Fluids, Mostly of Invariable Density," DTMB-NSRDC: Rept. 2299, Feb. 1967.
- ⁷Riabouchinsky, D., "Sur la resistance des fluides," *International Congress of Mathematics*, Strasbourg, 1920, C.R., p. 568.
- ⁸Taylor, J.L., "Hydrodynamical Inertia Coefficients," *Philosophical Magazine*, Vol. 9, 1930, p. 161.
- ⁹Lamb, Sir H., *Hydrodynamics*, 6th ed., Dover Publications, 1945.
- ¹⁰Sedov, L.I., "Two-Dimensional Problems of Gliding on the Surface of a Heavy Fluid," Transactions of the Conference of Wave Resistance, Moscow, U.S.S.R., 1937.
- ¹¹Squire, H.B., "The Motion of a Simple Wedge Along the Water Surface," *Proceedings of the Royal Society, Ser. A*, Vol. 243, 1957.
- ¹²Payne, P.R., "On High Efficiency Planing Surfaces and Their Spray Sheets," Payne, Inc., Working Paper 257-2, April 1979.
- ¹³Wadlin, K.L. and McGehee, J.R., "Planing Characteristics of Six Surfaces Representative of Hydro-Ski Forms," NACA RM L9L20, Feb. 1950.
- ¹⁴Payne, P.R., "The Lift on a Triangular Ski with Vertex Aft," Payne, Inc., Working Paper 268-14, Feb. 1980.
- ¹⁵Jones, R.T. and Cohen, D., *High Speed Wing Theory*, Princeton University Press, 1960.
- ¹⁶Wagner, H., "Landing of Seaplanes," NACA TM 622, 1931.
- ¹⁷von Kármán, T., "The Impact on Seaplane Floats During Landing," NACA TN 321, 1929.
- ¹⁸Korvin-Kroukovsky, B.V. and Chabrow, F.R., "The Discontinuous Fluid Flow Past an Immersed Wedge," Stevens Institute of Technology, Rept. 334, Oct. 1948.
- ¹⁹Pierson, J.D. and Leshnover, S., "A Study of the Flow, Pressures, and Loads Pertaining to Prismatic Vee-Planing Surfaces," Stevens Institute of Technology, Rept. 382, May 1950.
- ²⁰Sottorf, W., "An Analysis of Experimental Investigations of the Planing Process on the Surface of Water," NACA TM 1061, March 1944.
- ²¹Payne, P.R., "Supercritical Planing Hulls," AIAA Paper 74-333, presented at the AIAA/SNAME Advanced Marine Vehicles Conference, San Diego, Calif., Feb. 1974.
- ²²Payne, P.R., "Recent Developments with the Sea Knife," AIAA/SNAME Advanced Marine Vehicles Conference, Baltimore, Md., Oct. 1979.
- ²³Chambliss, D.B. and Boyd, G.M. Jr., "The Planing Characteristics of Two V-Shaped Prismatic Surfaces Having Angles of Deadrise of 20° and 40°," NACA TN 2876, 1953.
- ²⁴Sedov, L.I., *Two-Dimensional Problems in Hydrodynamics and Aerodynamics*, Interscience Publishers, N.Y., 1965.
- ²⁵Kapryan, W.J. and Boyd, G.M. Jr., "Hydrodynamic Pressure Distributions Obtained During a Planing Investigation of Five Related Prismatic Surfaces," NACA TN 3477, 1955.
- ²⁶Ferdinand, Jr. V., "Theoretical Considerations on the Penetration of a Wedge into the Water," *International Ship Building Progress*, Vol. 13, April 1966.
- ²⁷Pierson, J.D. and Leshnover, S., "An Analysis of the Fluid Flow in the Spray Root and Wake Regions of Flat Planing Surfaces," Stevens Institute of Technology, Rept. 335, Oct. 1948.
- ²⁸Payne, P.R., "On the Jet Thickness in High Speed Two-Dimensional Planing," *Journal of Hydronautics*, Vol. 14, No. 3, July, 1980.
- ²⁹Pabst, W., "Theory of the Landing Impact of Seaplanes," NACA TM 580, 1930.
- ³⁰Pabst, W., "Landing Impact of Seaplanes," NACA TM 624, 1931.
- ³¹Wagner, H., "Über Stoss- und Gleitvorgänge an der Oberfläche von Flüssigkeiten," *Z.f.a.M.M.*, Bd. 12, Heft 4, Aug. 1932.
- ³²Mewes, E., "Die Stosskräfte an Seeflugzeugen bei Starts und Landungen, Vereinigung für Luftfahrtforschung Jahrb., Berlin, R. Oldenburg, Munich, 1935.
- ³³Schmid, C., "Über den Landestoss von Flugzeugschwimmern," *Ing.-Archive*, Bd. X, Heft 1, Feb. 1939.
- ³⁴Sydow, J., "Über den Einfluss von Federung und Kielung auf den Landestoss Jahrb.," 1938 *der deutschen Luftfahrtforschung*, R. Oldenburg, Munich, 1938, pp. I 329-I 338 (available as British Air Ministry Translation 861).
- ³⁵Kreps, R.L., "Experimental Investigation of Impact in Landing on Water," NACA TM 1046, 1943.
- ³⁶Mayo, W., "Analysis and Modification of Theory for Impact of Seaplanes on Water," NACA TN 1008, Dec. 1945.
- ³⁷Pierson, J.D., "The Penetration of a Fluid Surface by a Wedge," Stevens Institute of Technology IAS Paper FF-3, July 1950.
- ³⁸Sottorf, W., "Experiments with Planing Surfaces," NACA TM 661, 1932.
- ³⁹Shoemaker, J.M., "Tank Tests of Flat V-bottom Planing Surfaces," NACA TN 509, Nov. 1934.
- ⁴⁰Bisplinghoff, R.L. and Doherty, C.S., "A Two Dimensional Study of the Impact of Wedges on a Water Surface," MIT Rept. Contract No(s) 9921, March 20, 1950.
- ⁴¹Monaghan, M.A., "Theoretical Examination of Effect of Deadrise in Seaplane-Water Impacts," Royal Aircraft Establishment TN Aero. 1989, 1949.
- ⁴²Zarnick, E.E., "A Nonlinear Mathematical Model of Motions of a Planing Boat in Regular Waves," DTNSRDC Rept. 78/032, March 1978.
- ⁴³Martin, M., "Theoretical Predictions of Motions of High Speed Planing Boats in Waves," *Journal of Ship Research*, Vol. 22, Sept. 1978.
- ⁴⁴Martin, M., "Theoretical Determination of Porpoising Instability of High-Speed Planing Boats," *Journal of Ship Research*, Vol. 22, March 1978.